Supplementary Figure 1

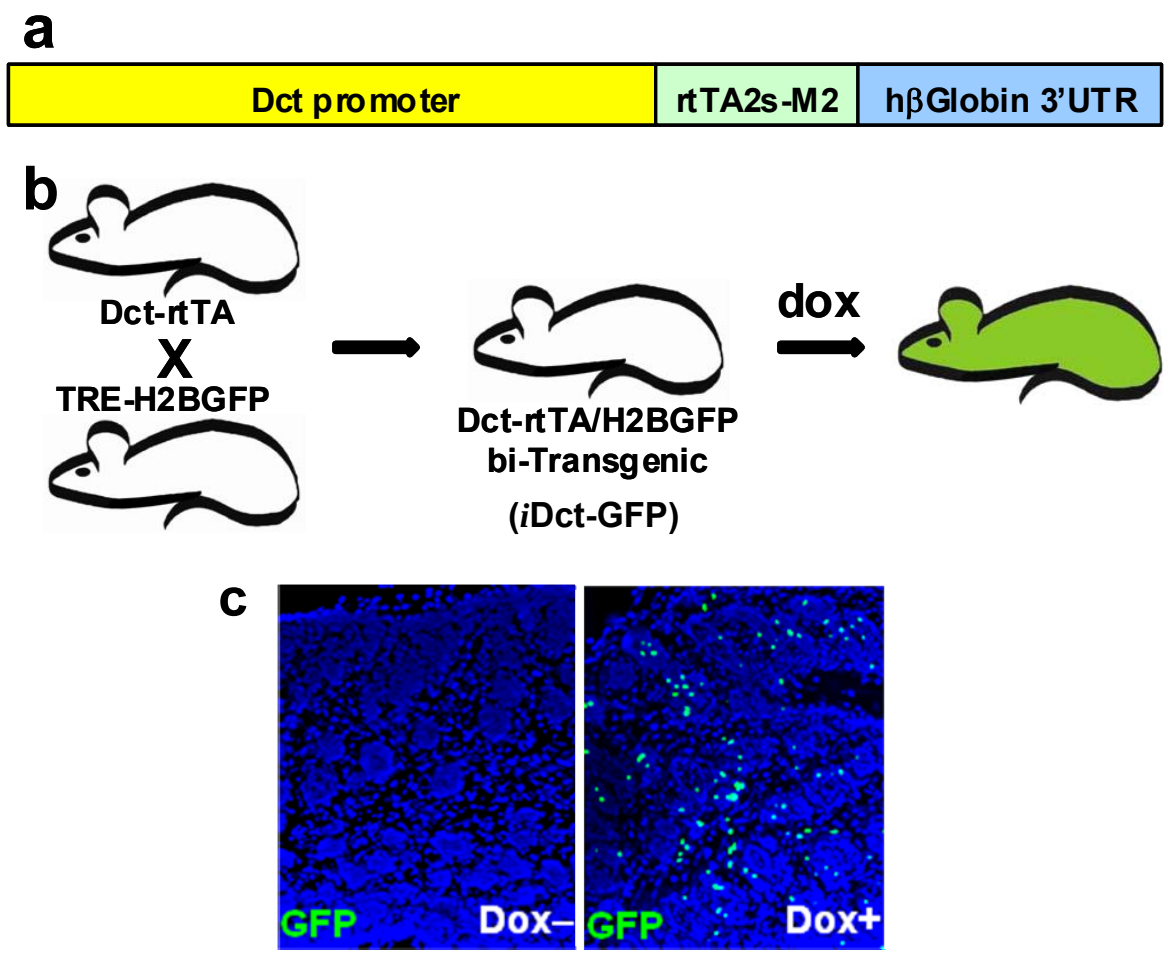

Supplementary Fig. 1. **a**, The transgene construct for making the Dct-rtTA mice. The 3.4 kb dopachrome tautomerase (*Dct*) gene promoter is melanocyte-specific. The rtTA2s-M2 version of the reverse tetracycline-activated transactivator provides leak-free expression and no background. The 3'UTR consists of partial exon 2, full intron 2 and exon 3 of human beta globin gene, and provides splice sites and an enhancer sequence for optimal transgene expression. Thirty-one transgenic founders were generated, of which one was selected for further studies. **b**, Dct-rtTA mice were bred with TRE-H2BGFP transgenic mice to produce *inducible* Dct-rtTA/TRE-H2BGFP double transgenic mice (*i*Dct-GFP), which expressed GFP exclusively in melanocytes when injected intraperitoneally with doxycycline (dox). **c,** *i*Dct-GFP mice show tight regulation of GFP expression in skin. No GFP expression is detectable in the absence of dox (left), but robust expression is seen within 12-18 hours of a single intraperitoneal injection of non-toxic dose of dox (right).

Supplementary Figure 2

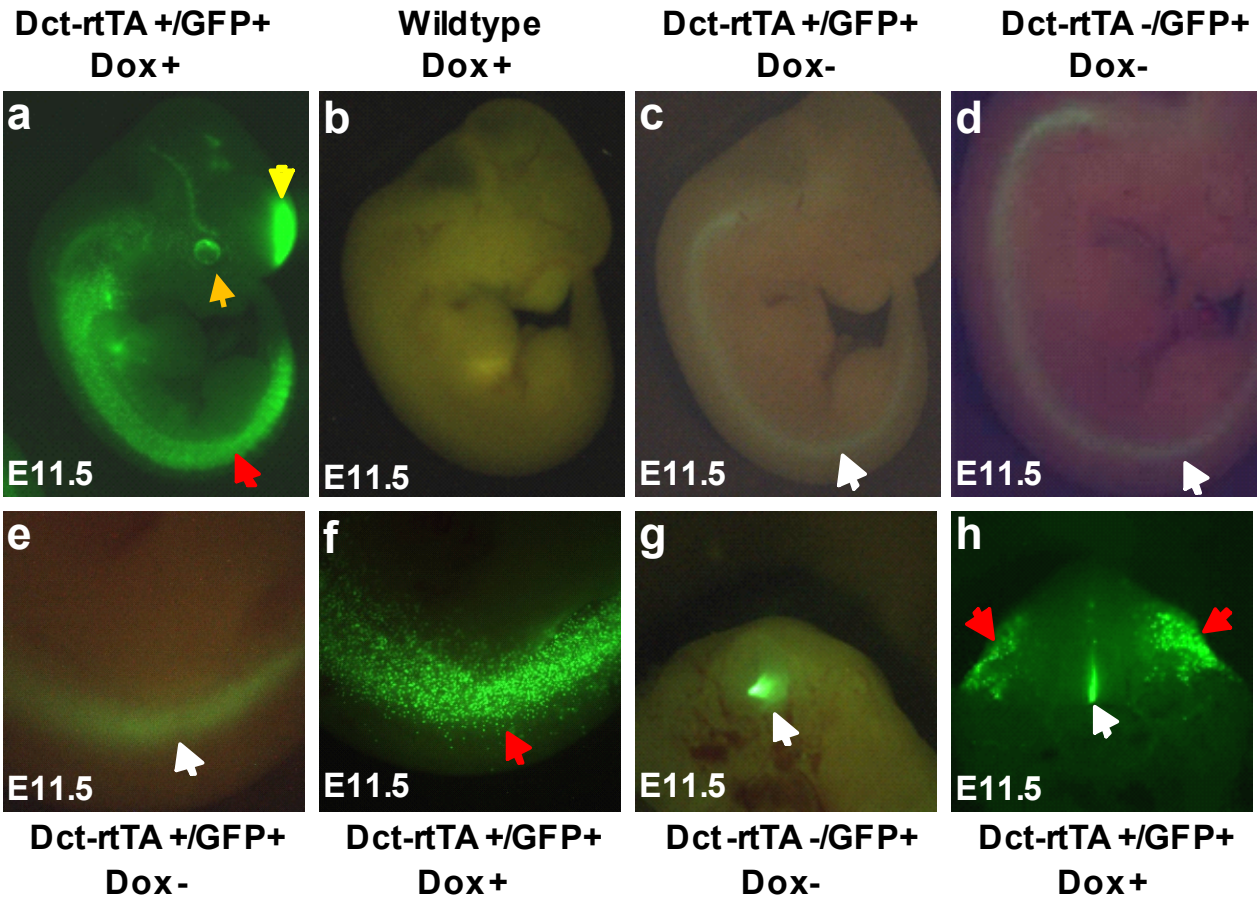

Supplementary Fig. 2. **a**, An E11.5 *i*Dct-GFP embryo showing GFP expression in the neural crest (red arrow), telencephalon (yellow arrow), and retinal pigment epithelium (orange arrow) after doxycycline (dox) administration to the mother. This expression pattern is in congruence with that of Dct as expected (Silver *et al.*, *Adv Exp Med Biol* 589:155-169). **b**, A wildtype control embryo shows no GFP expression. **c**, *i*Dct-GFP embryos without dox administration exhibit no GFP expression in neural crest, telencephalon or retinal pigment epithelium. However, there is a non-specific faint fluorescence in the floorplate (white arrow), which is also visible in the TRE-H2BGFP mice in the absence of dox (**d**). **e-f**, Floorplate shows non-specific faint fluorescence in the absence of dox (**e**), but dox induces GFP expression in the neural crest cells (**f**). **g**, A dorso-ventrally cut TRE-H2BGFP embryo shows non-specific fluorescence in the floorplate (arrow) in the absence of dox. **h**, A dorso-ventrally cut *i*Dct-GFP embryo after dox administration shows GFP+ melanoblasts moving dorso-laterally (red arrows), and non-specific floorplate fluorescence (white arrow).

Supplementary Figure 3

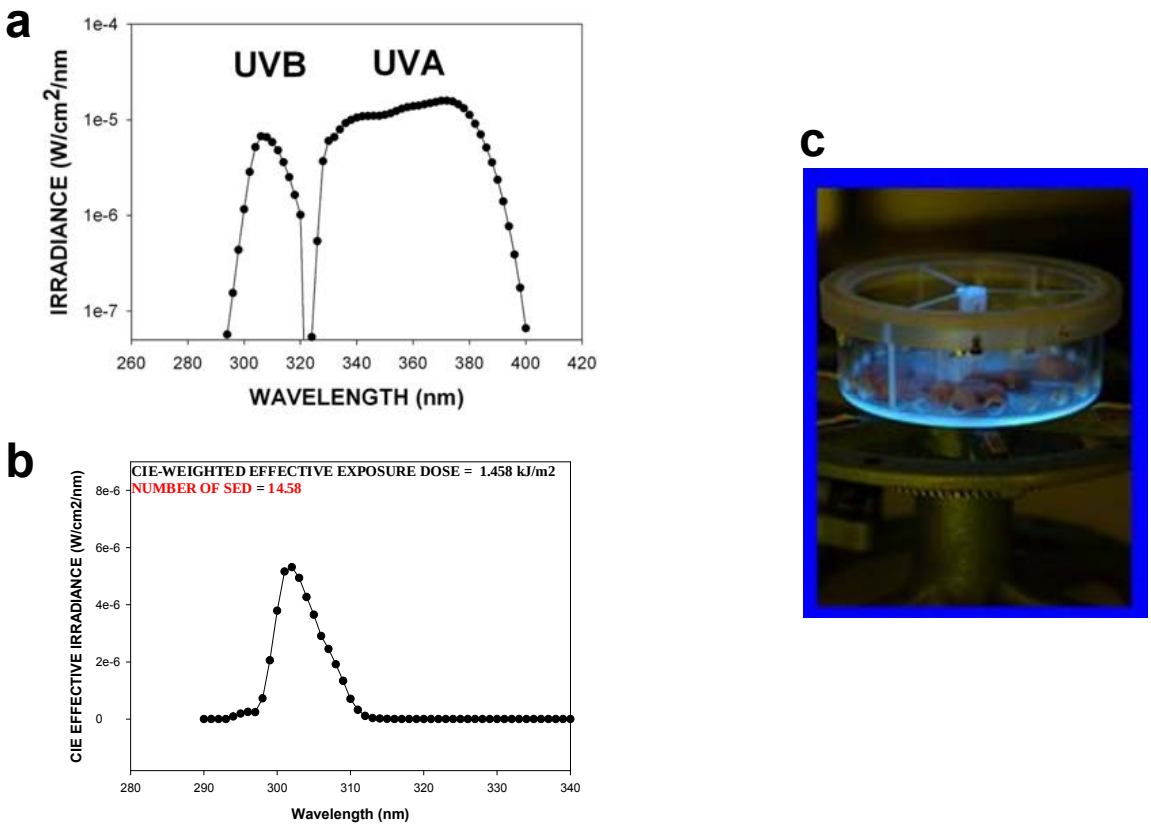

Supplementary Fig. 3. a, Interference filters with precisely defined wavebands of UVA (320-400 nm) or UVB (280-320 nm) radiation coupled to a 2.5 kW xenon arc created ~100 cm^2 of exposure area sufficient to expose all mice. As there is no melanoma "action" or wavelength dependent spectrum available for use in measuring melanoma-effective doses, we chose to use the CIE (Commission Internationale de l'Eclairage) erythemal or sunburn action spectrum (see Methods). **b,** The erythemal-effective dose delivered to neonatal mice from the UV source was calculated to be 15 Standard Erythemal Effective doses (SED). The absolute UVB dose delivered was 6 kJ/m^2 (output peak = 308 nm). In contrast, for UVA exposure, it was necessary to use the absolute rather than an erythemal-effective dose because UVA is far less effective than UVB in producing erythema. A dose of 150 kJ/m^2 (output peak = 375 nm) was delivered to the mice from the isolated UVA waveband. To put this in perspective, in sunlight, in mid-summer at Northern Hemisphere mid-latitudes between 11 am and 3 pm, 150 kJ/m^2 of UVA would have been received in approximately 50 minutes of sunlight exposure. In that time, an erythemal dose of about 7 SED would have been delivered, a dose we have previously determined to be melanomagenic (data not shown). **c**, Mice were irradiated in a specially designed module with a quartz lid, and three separate compartments capable of accommodating up to 12 neonates or 3 adult mice and evenly spaced air inlets around the module. The module sits on top of a rotating platform (3 RPM) to evenly distribute the circular UV beam to all compartments.

Supplementary Figure 4

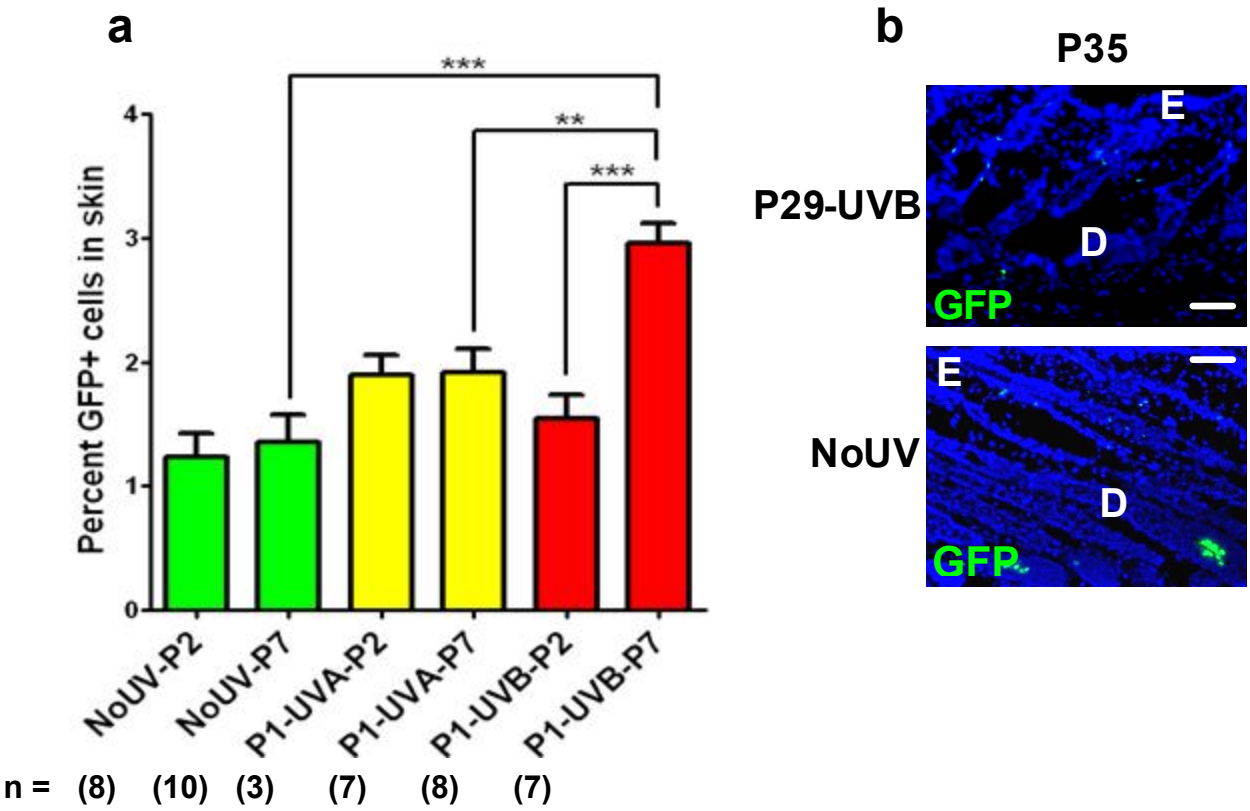

Supplementary Fig. 4. a, Percentage of GFP+ melanocytes in single cell suspensions made from back skins of neonatal *i*Dct-GFP mice at ages of 2 days (P2) and 7 days (P7), following irradiation at P1 with either UVA or UVB. No statistical differences in the GFP+ melanocytic populations were seen among the unirradiated and UVA-irradiated pups at either P2 or P7. However, UVB-irradiated pups exhibited statistically significant increase (~2-fold) in GFP+ melanocytes at P7, as compared with the unirradiated control and UVA-irradiated P7 pups. For each group, the indicated number of biological replicates (n) were quantified via flow cytometry. Every replicate consisted of back skins pooled from 6-8 pups. **P<0.01; ***P<0.001; Student's t-test. **b,** UVB did not activate melanocytes in adult mice irradiated at P29 and examined at P35. Blue = DAPI. E = epidermis; D = dermis. Scale bars = 40 μm.

Supplementary Figure 5

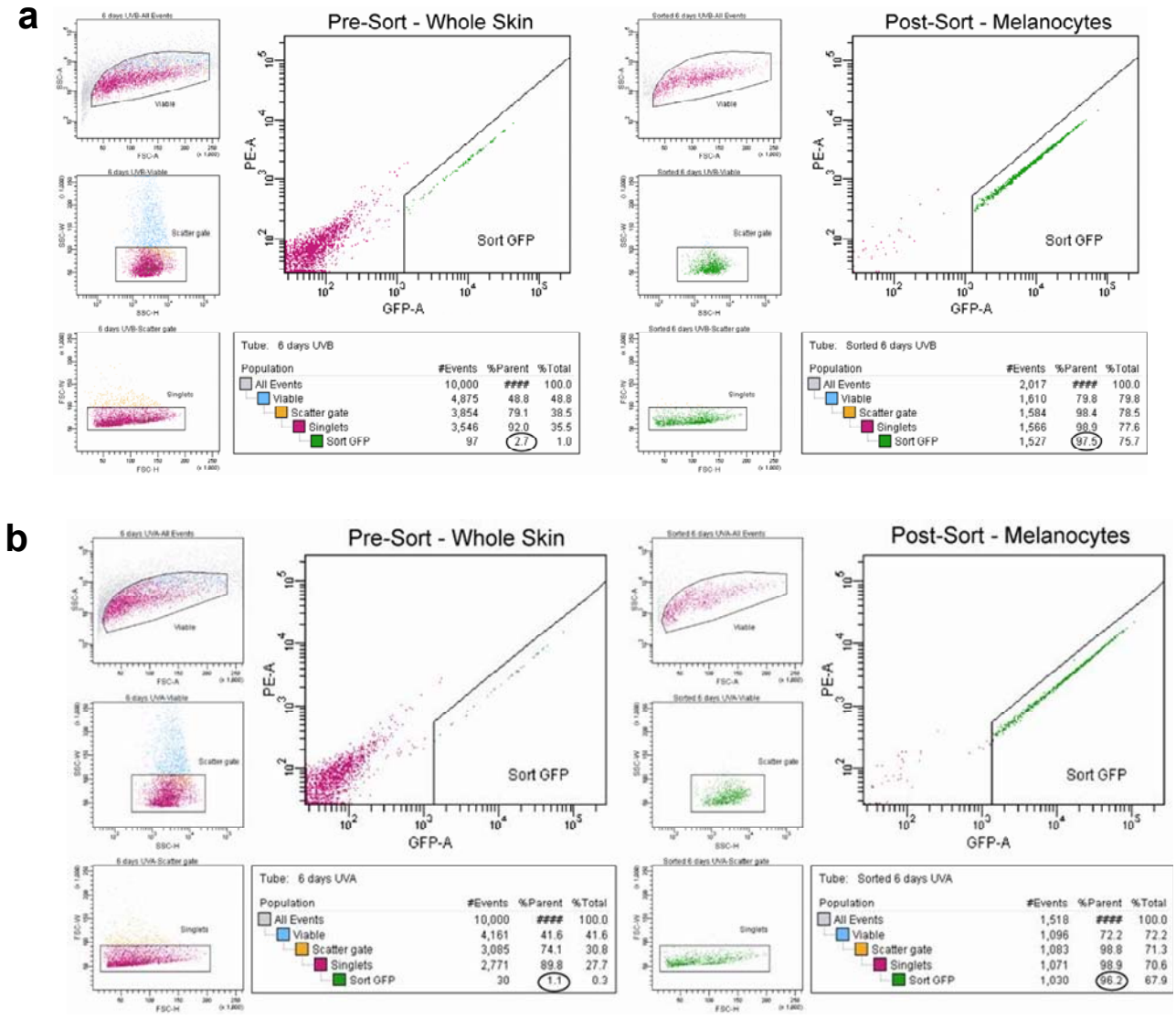

Supplementary Fig. 5. Representative FACS sorting schemes are shown for isolation of GFP+ melanocytes from UVB (**a**) and UVA (**b**) irradiated *i*Dct-GFP pup skins at 6 days post irradiation (P7). Pre-sort analyses of the whole skin cell suspensions (left panels) showed 1-2% GFP+ cells in the UVA irradiated skins (equivalent to unirradiated controls), but an elevated 2.5-3.5% GFP+ cells in the UVB-irradiated pups (circled). Post-sort analyses (right panels) showed high enrichment (>95%, circled) of GFP+ melanocytes.

Supplementary Figure 6

a

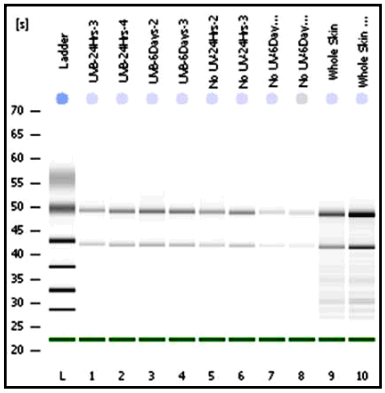

b

Gene	Expression intensity
Dct	27,273
Melan-A	24,141
Silver	18,024
Tyrp1	14,224
Keratin 1	54
Keratin 10	158
αSMA	50
Fabp4	44

Supplementary Fig. 6. **a,** Bioanalyzer analysis of the total RNA extracted from the FACS-sorted GFP+ melanocytes showed high quality RNA. **b,** cDNA microarray analysis of gene expression showed that the FACS-sorted GFP+ cells were indeed highly pure melanocytes. The expression intensities detected on the microarray for melanocyte-specific genes (red) were extremely high and represented among the highest detected gene intensities on the array; Dct was in fact the highest. In contrast, expression of keratinocyte-specific (Keratin 1 and Keratin 10), fibroblast-specific (alpha smooth muscle actin), and adipocyte-specific (Fabp4) genes were below the threshold of detection. This proved that the FACS-sorted GFP+ cells were highly pure melanocytes and were devoid of contamination from other cell types found in the cellular milieu of the mouse skin.

Supplementary Figure 7

Expanded view of Figure 3a with gene names; top 205 most statistically significant genes.

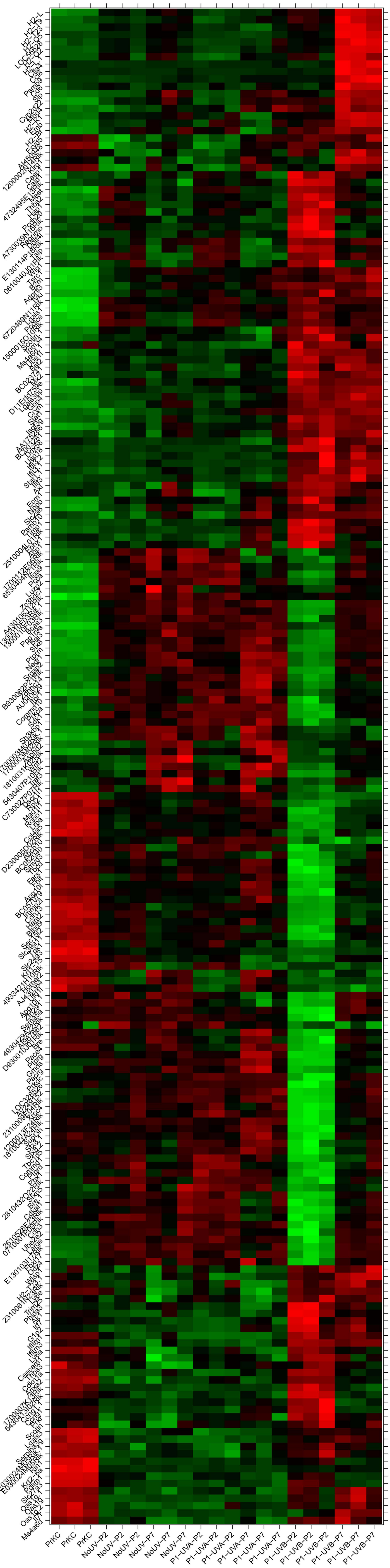

Supplementary Figure 8

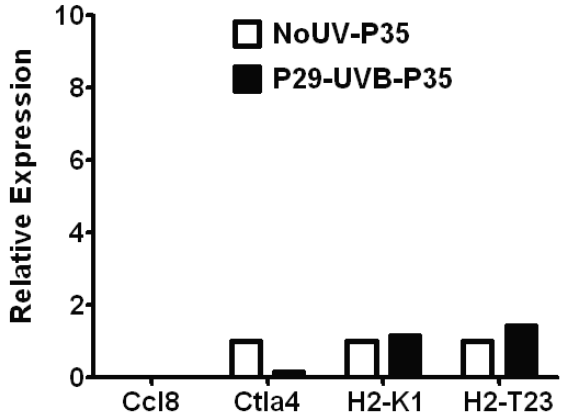

Supplementary Fig. 8. In order to determine whether the adult skin melanocytes exhibit the same gene expression response to UVB as the neonatal skin melanocytes, adult *i*Dct-GFP mice were UVB-irradiated at age P29, and melanocytes were FACS-isolated 6 days later at P35. qRT-PCR analysis of the indicated genes showed no upregulation in adult skin melanocytes in response to UVB irradiation, as compared to the unirradiated controls.

Supplementary Figure 9

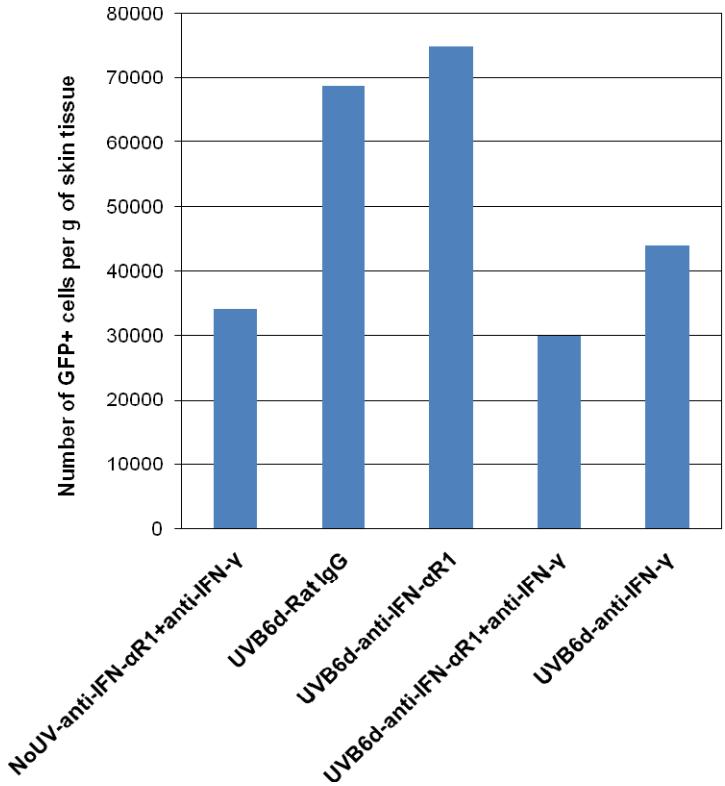

Supplementary Fig. 9. The ability of antibody (Ab)-mediated blockade of Type-I and Type-II interferons to inhibit the UVB-induced neonatal skin melanocyte activation was tested. Pooled back skins from 5-6 pups were used per group. The *i*Dct-GFP pups were administered anti-IFN-αR1 (to block IFN-α and IFN-β), anti-IFN-γ, or both antibodies, 1 hour prior to, and 3 days after UVB-irradiation. Rat IgG isotype antibody was used as control. Six days following UVB-irradiation (UVB6d), the back skins were harvested, weighed, single-cell suspensions were made, and GFP+ melanocytes were FACS-isolated and quantified per gram of skin tissue. As expected, the UVB-irradiated skins with Rat IgG isotype Ab treatment yielded twice the number of GFP+ cells as compared to the unirradiated controls with dual Ab treatment (NoUV-anti-IFN-αR1+anti-IFN-γ). Single Ab treatment with anti-IFN-αR1 Ab failed to affect the GFP+ cell yield. However, dual treatment with anti-IFN-αR1+anti-IFN-γ and single treatment with anti-IFN-γ Ab reduced the GFP+ cell yield by 44-57%, to levels comparable to the unirradiated skin. This showed that blockade of IFN-γ dramatically inhibited the UVB-induced melanocyte activation.

Supplementary Figure 10

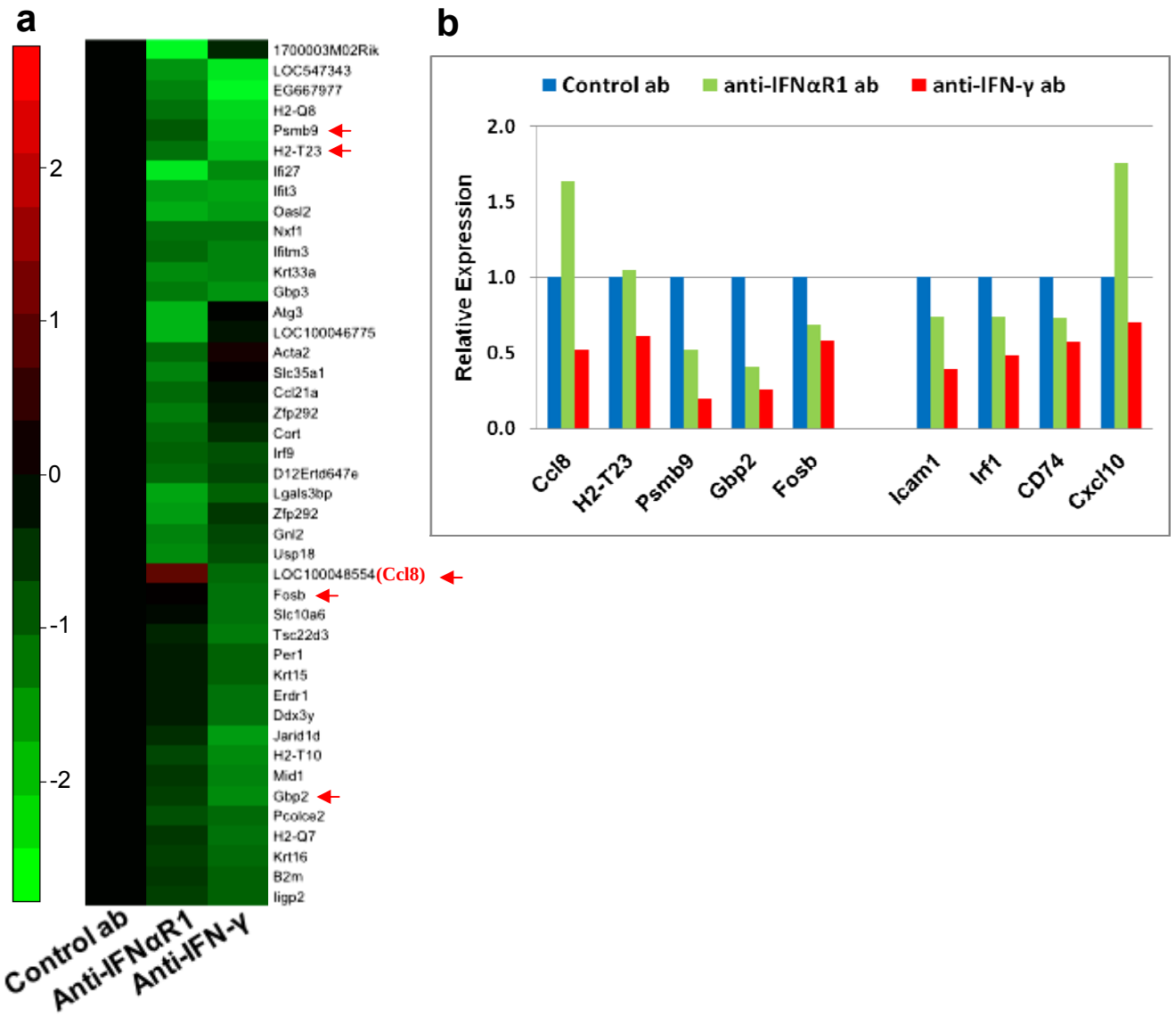

Supplementary Fig. 10. In order to delineate IFN Type-I and Type-II specific gene expression response to UVB, *i*Dct-GFP pups were administered anti-IFN-αR1 (to block type-I IFN) or anti-IFN-γ antibodies, 1 hour prior to, and 3 days after UVB irradiation. Rat IgG isotype (clone GL113) antibody was used as control. Six days following irradiation, GFP+ melanocytes from back skins (pooled from 6 pups for each sample) were FACS-isolated, and cDNA microarrays were performed. **a,** Heatmap of unsupervised clustering of genes that were >1.5-fold changed in either anti-IFN antibody-treated sample as compared to the control antibody-treated sample. As expected, a subset of genes was concurrently downregulated by both Type-I and Type-II IFN blockade. In addition, Type-I- and Type-II-specific genes were also evident. **b,** qRT-PCR validations were performed for 5 select genes indicated in the heatmap (red), as well as for four other known IFN-responsive genes (rightmost 4).

Supplementary Figure 11

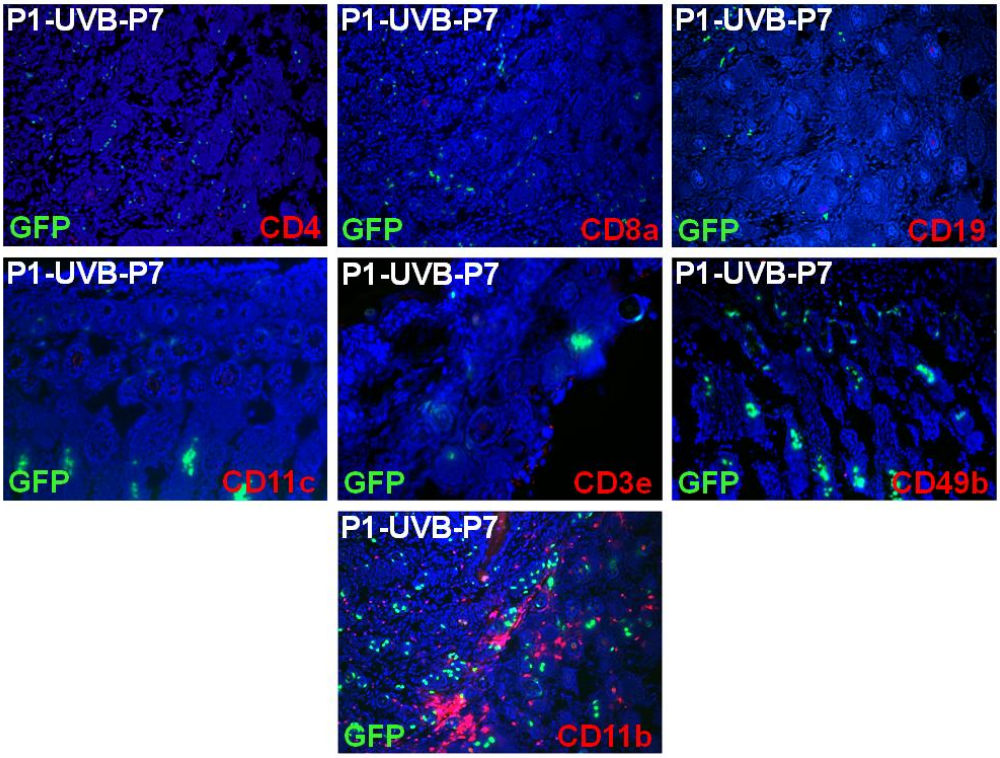

Supplementary Fig. 11. Immunohistochemical (IHC) analyses for a variety of immune cell types in *i*Dct-GFP neonatal skins that were UVB-irradiated at P1 and harvested at P7. IHC with anti-CD4 (T cell-specific), anti-CD8a (T cells), anti-CD19 (B cells), anti-CD11c (dendritic cells), anti-CD3e (NK-T cells), and anti-CD49b (DX5; natural killer cells) showed no immunostaining. However, a substantial number of CD11b+ cells (myeloid cells) were readily identifiable.

Supplementary Figure 12

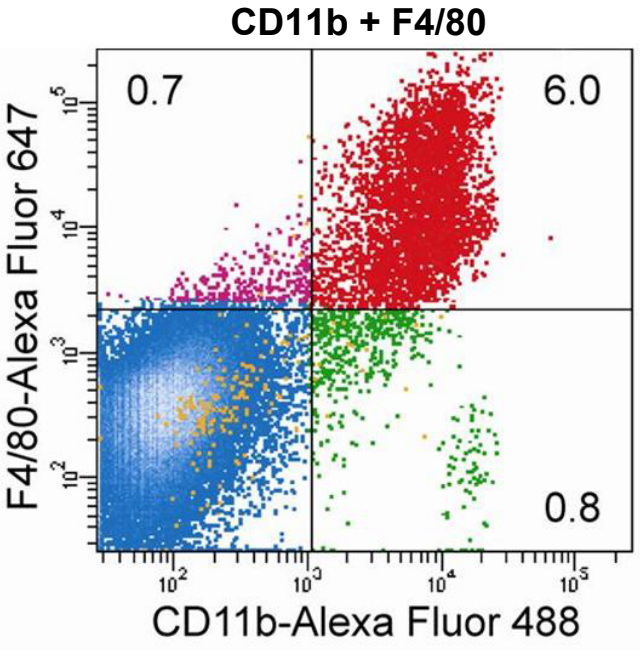

Supplementary Fig. 12. Dual fluorescence flow cytometry analysis of single-cell suspensions from back skins of *i*Dct-GFP pups UVB-irradiated at P1 and harvested at P7 showed that 90% of the CD11b+ cells were also F4/80+, identifying them as macrophages. For this experiment, GFP expression was kept off by not administering dox to the *i*Dct-GFP mice, which allowed use of Alexa Fluor 488-labeled anti-CD11b antibody.

Supplementary Figure 13

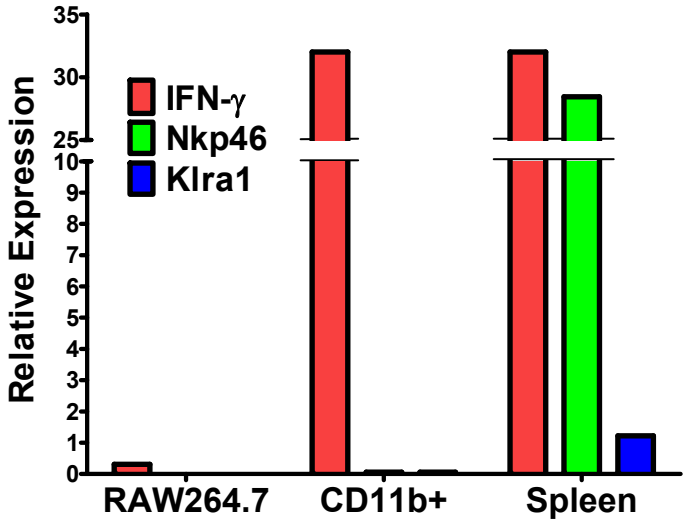

Supplementary Fig. 13. Natural killer (NK) cells are not detectable in the FACS-isolated, UVB-recruited skin CD11b+ population. In order to determine whether the CD11b+ population FACS-isolated from skin 6-days post UVB irradiation (irradiation at P1, isolation at P7), which show highly upregulated expression of IFN-γ, may be contaminated with NK cells, we performed qRT-PCR for two NK cell markers, NKp46 and Klra1 on the CD11b+ population. We were unable to detect any expression of either of these two NK cell markers in the CD11b+ population. Whole spleen was used as a positive control.

Supplementary Figure 14

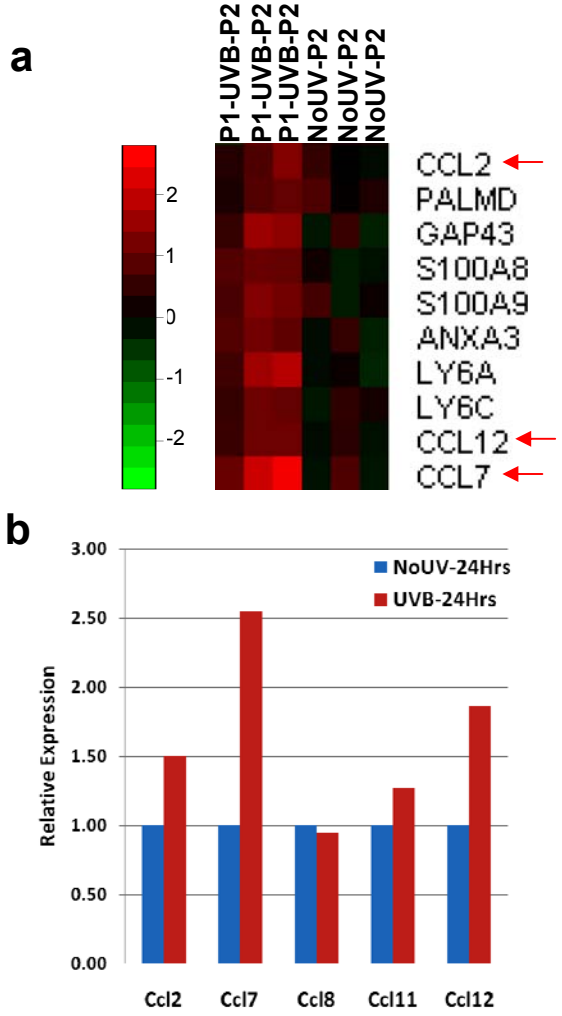

c

Gene Symbol	Fold Regulation	Gene Symbol	Fold Regulation
Bdnf	2.1644	Cx3cl1	2.4351
Bmp10	2.1126	Cxcl1	9.6398
Ccbp2	2.4777	Cxcl10	50.8791
Ccl1	2.3768	Cxcl11	3.8611
Ccl11	2.385	Cxcl12	5.5174
Ccl12	60.2964	Cxcl13	2.574
Ccl17	2.9773	Cxcl2	28.4233
Ccl19	2.619	Pf4	2.2879
Ccl20	11.7452	Cxcl5	5.0771
Ccl4	2.4183	Ppbp	3.2132
Ccl5	8.3051	Cxcl9	7.7758
Ccl7	2.1199	Cxcr4	4.0812
Ccl8	25.5278	Cxcr6	2.1199
Ccl9	2.0763	Gdf5	2.5562
Ccr1l1	3.338	Ccr10	2.2721
Ccr4	3.093	Gpr81	3.8879
Ccr6	3.8344	Il18	2.4267
Ccrl1	3.3035	Il1a	4.3289
Ccrl2	14.8151	Il8ra	3.1253
Cmtm2a	5.2018	Myd88	4.299
Cmtm3	2.0265	Tnf	4.5916
Cmklr1	2.1644	Trem1	5.7717
Cxcr7	12.5012	Xcl1	2.2958
Csf1	5.1301	Il8rb	-3.4846
Csf2	20.3083	Slit2	-5.2817

Supplementary Fig. 14. **a,** Partial heatmap depicting unsupervised hierarchical clustering of cDNA microarray data of 24 hrs post UVB irradiated and the unirradiated control samples. Three of the Ccr2/Ccr5 ligand chemokines (red arrows) show upregulated expression in the UVB-irradiated samples as compared to the unirradiated control samples. **b,** qRT-PCR validation for the Ccr2/Ccr5 ligands was performed on FACS purified melanocytes from back skins of pups UVB-irradiated at P1 and harvested 24 hrs later. Unirradiated pups of same age were used as controls. Means of two experiments are plotted, with each experiment containing pooled skins from 6-8 pups. **c,** RT^2 Profiler PCR Array (SABiosciences, Inc.) for mouse chemokines and receptors (PAMM-022A; 84 genes) was performed on total RNA isolated from the melan-c melanocyte cell line that was UV-irradiated by FS20 sunlamps and harvested 24 hrs later. 48 genes were upregulated (red) and only 2 downregulated (green) >2-fold as compared to the unirradiated controls. The ligands for Ccr2/Ccr5 are highlighted in yellow. It should be noted that Ccr2 can also bind at relatively low affinity human beta-defensin-2 and -3 (in mouse -4 and -14) (Rohrl *et al., J Immunol* 184:6688-6694), which can be released following UV exposure (Glaser *et al., J Allergy Clin Immunol* 123:1117-1123).

Supplementary Figure 15

RT^2 qPCR Array 24 Hrs post UVB irradiation in whole skin

a

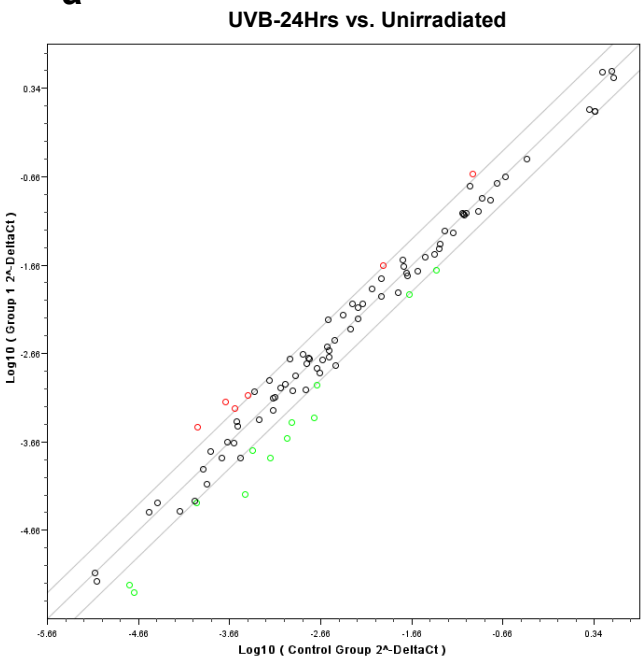

b

Gene Symbol	Fold Regulation
Cxcl1	3.1738
Cxcl13	2.1416
Pf4	2.2953
Cxcl5	3.3606
Il1a	2.0191
Il8rb	2.0975
Bmp6	-2.0157
Ccr4	-2.8606
Ccr6	-4.4654
Ccr8	-5.811
Ccrl1	-2.1381
Cxcl10	-3.8806
Cxcl15	-4.5121
Cxcl9	-2.0652
Tnfsf14	-2.2639
Xcl1	-4.1881

Supplementary Fig. 15. RT^2 Profiler PCR Array (SABiosciences, Inc.) for mouse chemokines and receptors (PAMM-022A; 84 genes) was performed on total RNA isolated from whole skin (~85% keratinocytes) samples from pups that were UVB-irradiated at P1 and harvested 24 hours later (n=4). Unirradiated pups of same age were used as controls (n=4). **a,** Scatter plot depicting comparison of mean expression levels of the 84 genes profiled, with a 2-fold cut-off threshold. **b,** Six genes were upregulated (in red) and 10 were downregulated (green) >2-fold in the UVB-irradiated skin samples as compared to the unirradiated controls. None of the upregulated genes were known to be chemoattractants for macrophages.

Supplementary Figure 16

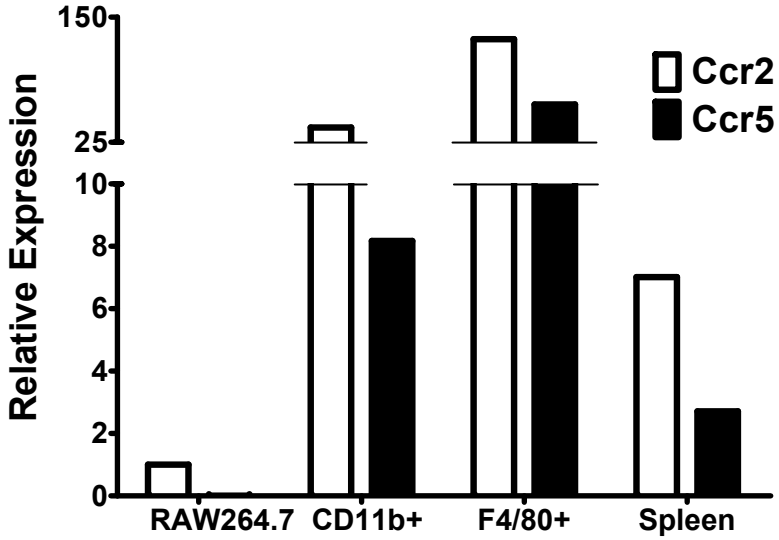

Supplementary Fig. 16. qRT-PCR analyses for Ccr2 and Ccr5 (receptors for Ccl8) were performed on CD11b+ and F4/80+ cells isolated from P1-UVB-P7 skin samples by immunofluorescence-FACS sorting. Non-activated RAW264.7 macrophage cell line was included as a positive control, as this cell line expresses Ccr2 and Ccr5 at baseline levels with Ccr2 being expressed at approximately 100-fold higher levels than Ccr5. Both CD11b+ and F4/80+ neonatal skin cells highly expressed Ccr2 and Ccr5 relative to non-activated RAW264.7 macrophages.

Supplementary Figure 17

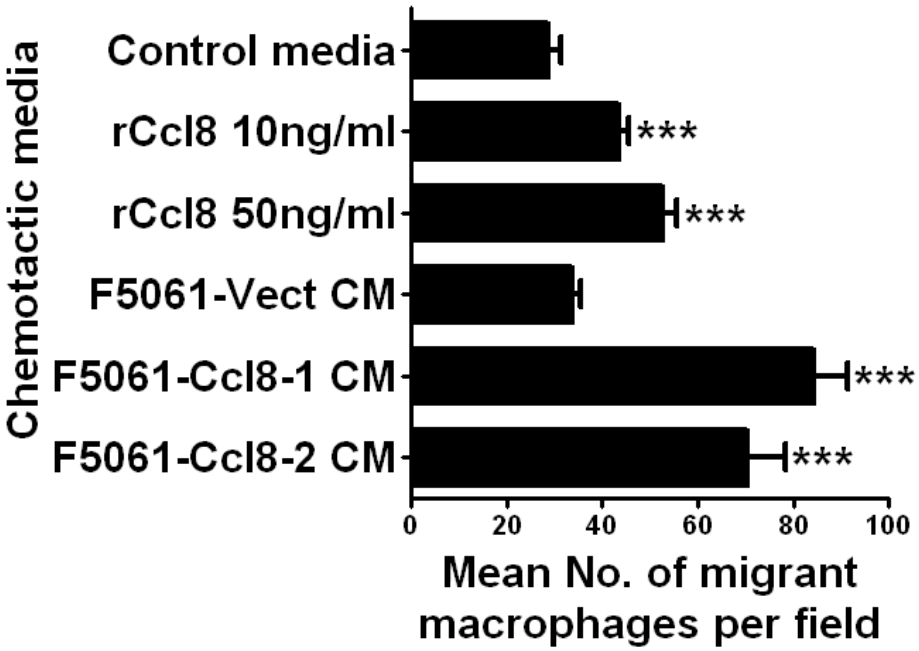

Supplementary Fig. 17. Boyden chamber chemotactic assay with conditioned media (CM) from Ccl8-transfected or vector-transfected F5061 melanoma cells (a cell line established from a UVB-induced melanoma in our HGF/SF transgenic mouse model). Recombinant mouse Ccl8 (rCcl8) in indicated concentrations was used as positive control. Migration of RAW264.7 macrophage cells was quantified in duplicate with 5 random fields observed per chamber. Mean number of migrant cells per field ±s.e.m. are depicted. ***p<0.001, One-Way ANOVA test with post-hoc Tukey analysis. The results confirm that Ccl8 is a potent macrophage chemoattractant (Van Damme *et al., J Exp Med* 176:59-65).

Supplementary Figure 18

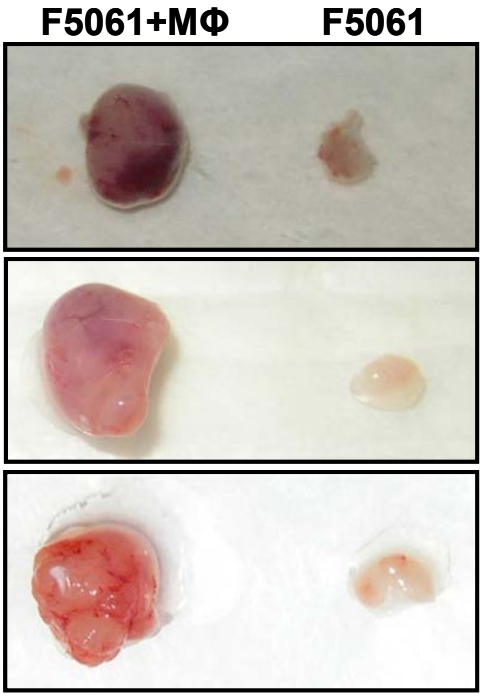

Supplementary Fig. 18. Macrophages (MΦ) recruited to the skin after UVB irradiation are pro-tumourigenic. F4/80^{+} macrophages were FACS-isolated from P1-UVB-P7 pup skins, and admixed with the F5061 cells (a cell line established from a UVB-induced melanoma in our HGF/SF transgenic mouse model) in a 1:5 ratio (50,000 MΦ + 250,000 F5061) and inoculated subcutaneously in syngeneic FVB/N mice (n=10). Control mice were inoculated with 250,000 F5061 cells only (n=10; one mouse died prematurely and was removed from the analysis). The experiment was performed in three different batches. The experiments were terminated 3 weeks after inoculation and tumour volumes were measured as described in Methods. Representative pairs of admixed and control tumours are shown from the three experiments, clearly demonstrating a growth advantage to the F5061+ MΦ admixed tumours.

Supplementary Figure 19

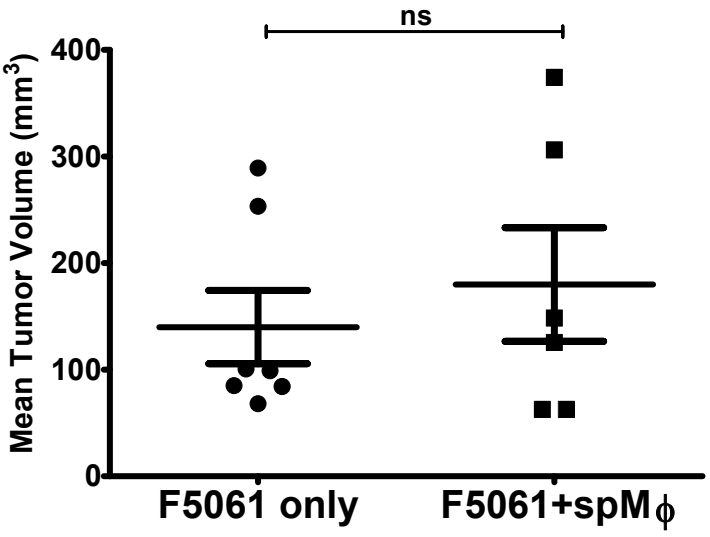

Supplementary Fig. 19. Macrophages isolated from spleens (spMΦ) of unirradiated pups did not significantly affect the growth of subcutaneously transplanted F5061 melanoma cells. F4/80+ spleenic macrophages were isolated by FACS from single-cell suspensions made from spleens of unirradiated 7-day old pups. These spMΦ were admixed with F5061 cells in a 1:5 ratio (50,000 MΦ + 250,000 F5061) and inoculated subcutaneously in syngeneic FVB/N mice (n=6). Control mice were inoculated with 250,000 F5061 cells only (n=7). The experiment was terminated 3 weeks after inoculation, and tumor volumes were measured. p = 0.52, Student's t-test. ns = not significant.

Supplementary Figure 20

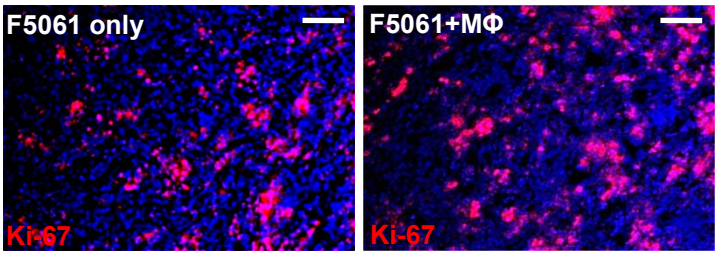

Supplementary Fig. 20. The F5061+ MΦ admixed tumours and the F5061 only control tumours exhibited equivalent Ki-67 immunohistochemical positivity (n=6 each group). Representative photomicrographs are shown. These results show that differential growth of these two tumour groups is not due to differences in cellular proliferation. Scale bars = 60 μm.

Supplementary Figure 21

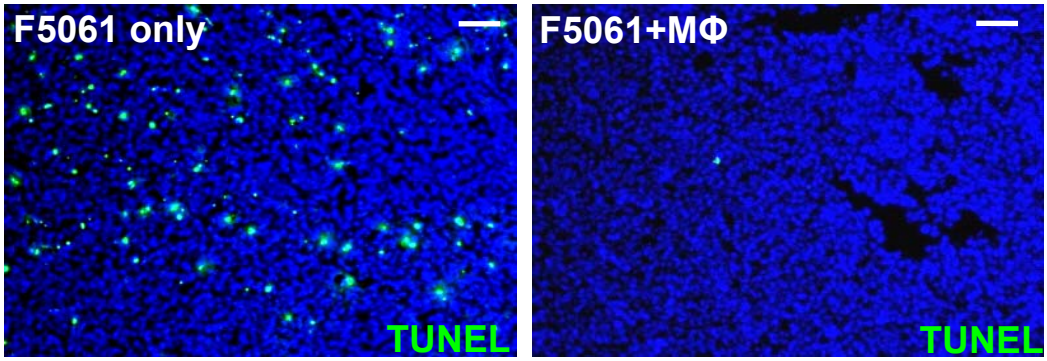

Supplementary Fig. 21. Fluorescence-based TUNEL assay showed dramatically different levels of apoptosis between F5016+MΦ admixed and control tumors (n=6 each). The apoptosis levels were significantly lower in the admixed tumors than in the control tumours. Representative photomicrographs are shown. Scale bars = 40 μm.

Supplementary Figure 22

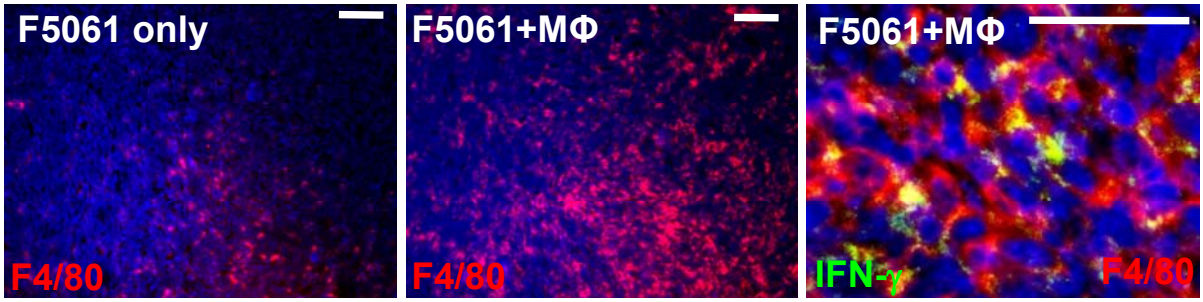

Supplementary Fig. 22. IHC analysis for presence of macrophages in control (F5061 only; left panel) and admixed (F5061+MΦ; middle panel) tumours. The survival advantage in the admixed tumours coincided well with the continued presence of macrophages in the admixed tumours; in fact, the number of tumour-associated macrophages was overtly greater than the original number of macrophages transplanted, indicating recruitment by positive feedback. Anti-F4/80 and anti-IFN-γ dual IHC showed that a subset of these macrophages expressed IFN-γ (right panel; yellow merged signal). Scale bars = 40 μm and 130 μm.

Supplementary Figure 23

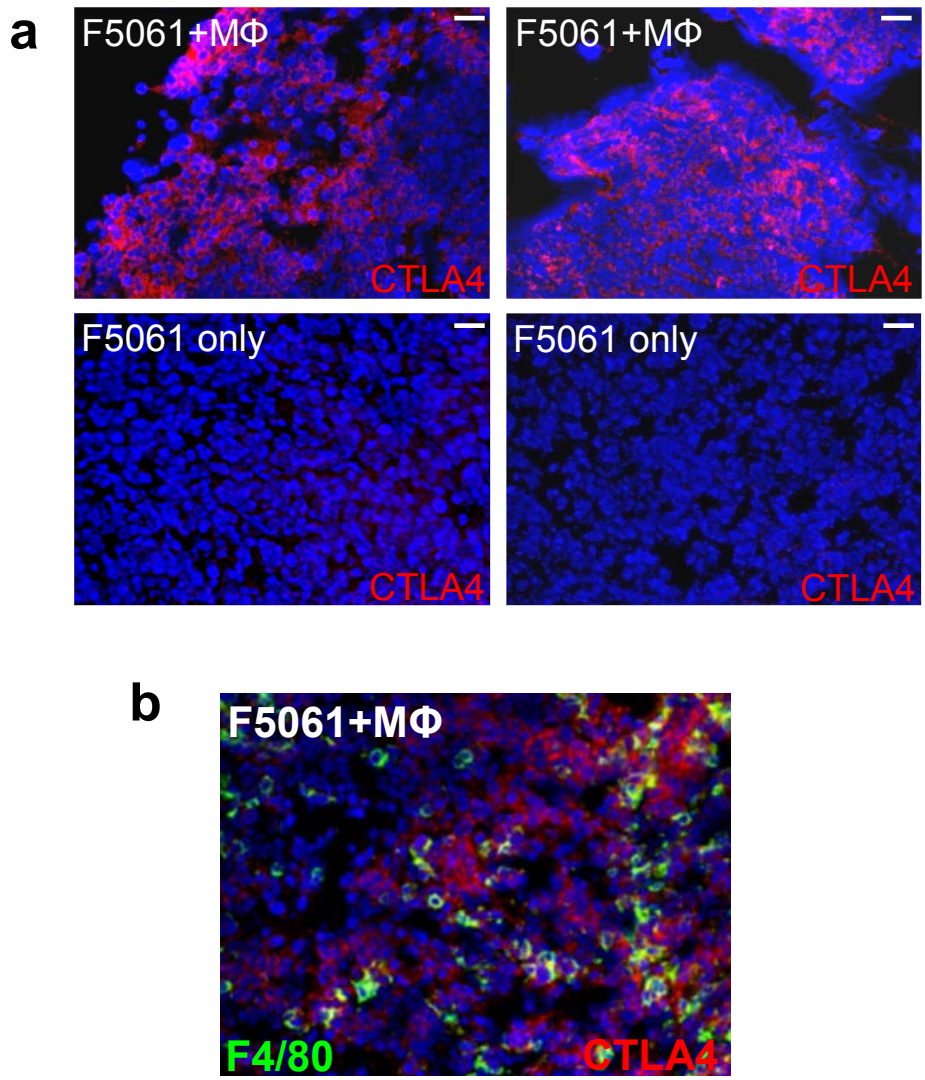

Supplementary Fig. 23. a, Since CTLA4 has been shown to be positively regulated by IFN-γ (e.g. Wong *et al.*, Journal of Investigative Dermatology 126:212, 2006), we tested whether CTLA4 was upregulated in the tumours with admixed skin macrophages. The F5061+MΦ admixed tumours exhibited high levels of CTLA4 immunopositivity. All 6 of 6 admixed tumours examined were positive for CTLA4. In contrast, only 1 of 6 F5061 only control tumours (lower left panel) showed faint positivity for CTLA4, while all others were negative. Representative photomicrographs are shown. Scale bars = 40 μm. **b,** Dual IHC with anti-F4/80 (green) and anti-CTLA4 (red) antibodies shows CTLA4 expression predominantly in melanoma cells but not in macrophages.

Supplementary Figure 24

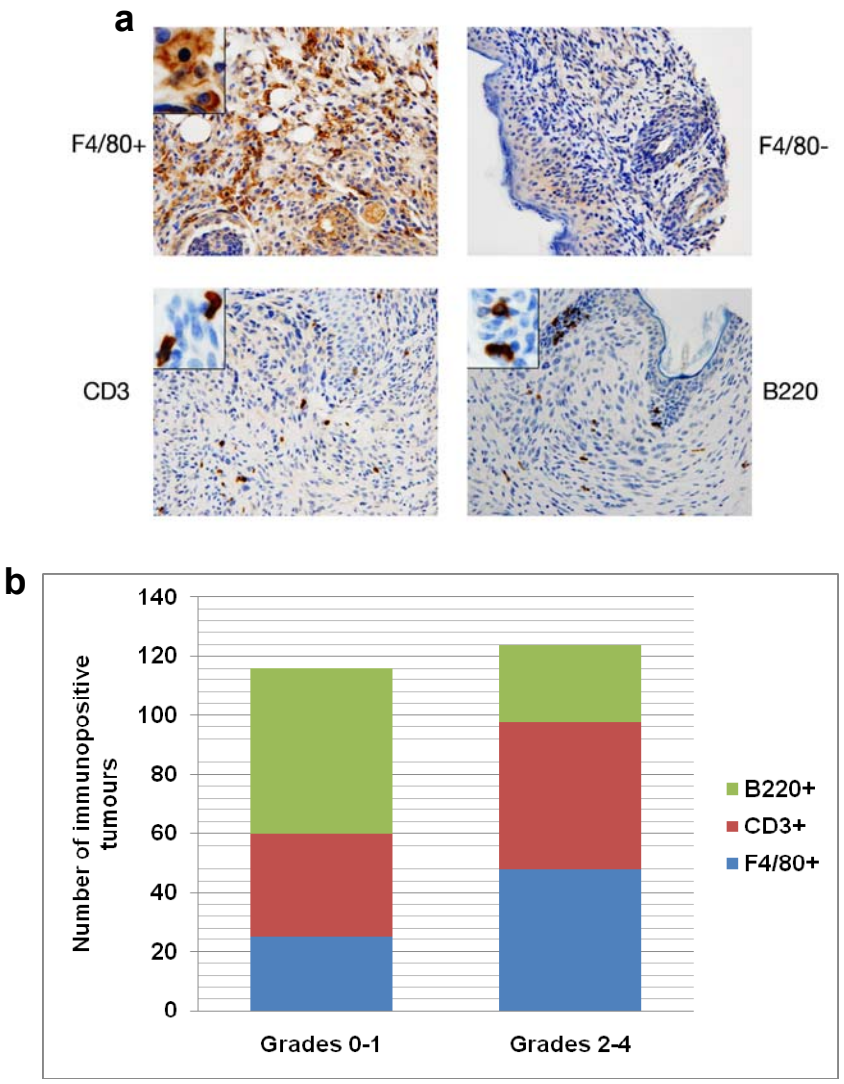

Supplementary Fig. 24. **a**, Immunohistochemical staining for F4/80 (macrophage marker), CD3 (T cell marker) and B220 (B cell marker) were performed on a tissue microarray (TMA) of UVB-induced melanomas from our albino HGF/SF transgenic mouse model. Immunostaining was evaluated according to the following grading system: 0=negative, 1=minimal, 2=mild, 3=moderate, and 4=severe. Representative photomicrographs (10x) are shown with high magnification insets (100x). **b**, Graphical representation of the number of tumours that were found to be either negative-minimally positive (grades 0-1) or mild-strongly positive (grades 2-4).

Supplementary Figure 25

a

Human Melanoma Tissue Microarray	
Melanomas on the array	27
CD68–	8
CD68+	19
CD68+IFN-g+	19

b

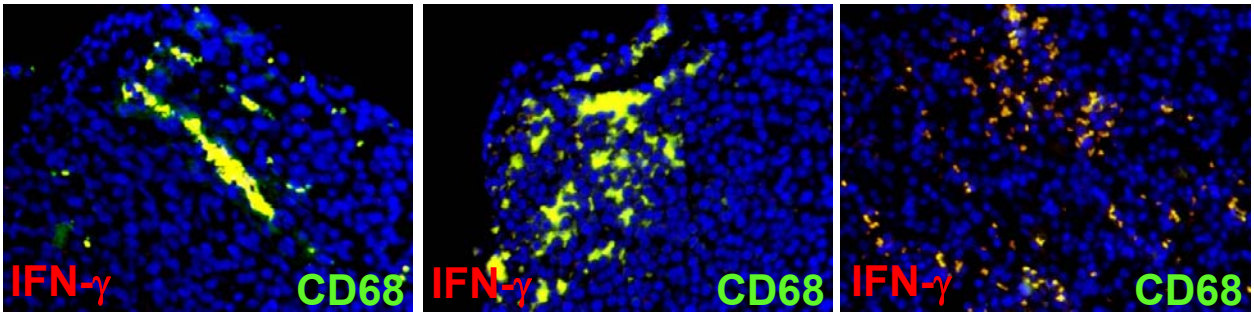

Supplementary Fig. 25. Dual immunohistochemistry with anti-CD68 (green) and anti-IFN-γ (red) antibodies on a human melanoma tissue microarray (TMA) showed tumour-associated macrophages expressing IFN-γ. **a**, Details of the human melanoma TMA. The TMA included 11 primary, 7 lymph node metastases, 5 distant metastases, and 4 human melanoma cell line xenografts. **b**, Three different representative human melanomas from the TMA show co-immunostaining of CD68 and IFN-γ (yellow).

Supplementary Figure 26

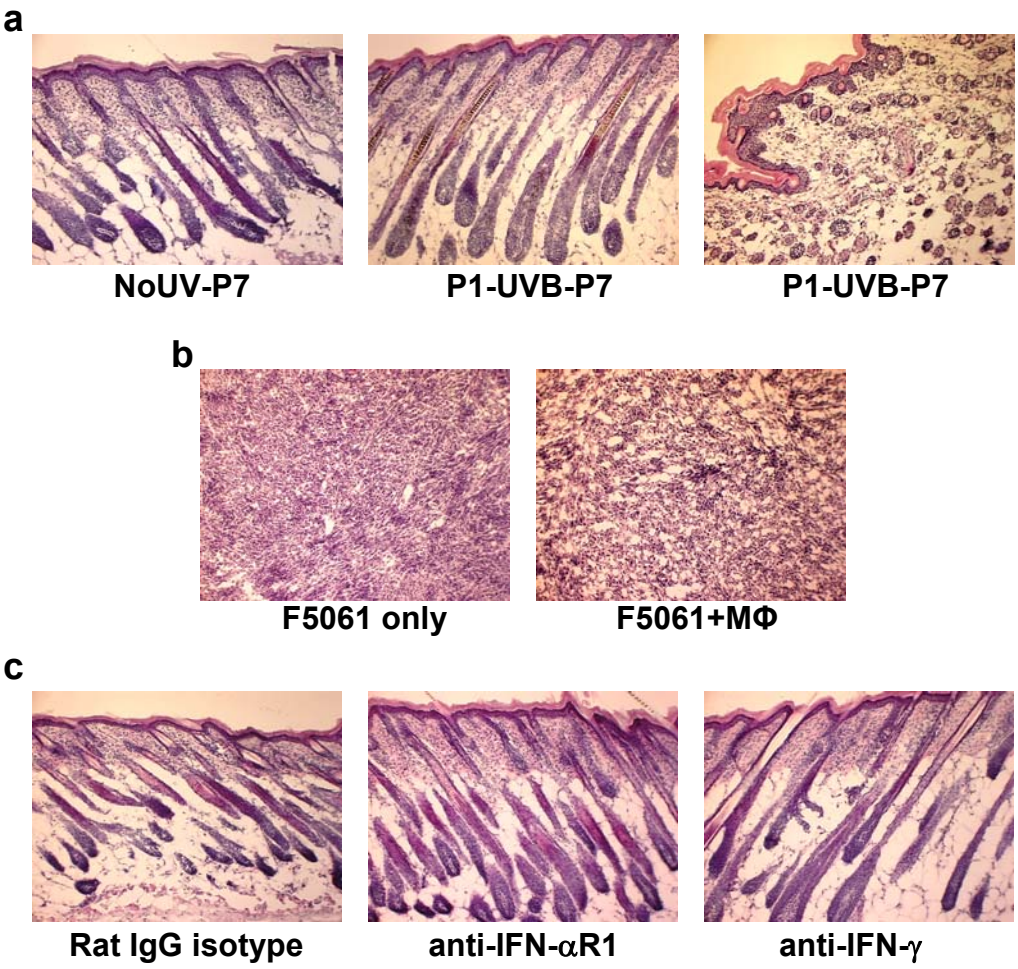

Supplementary Fig. 26. Representative hematoxylin & eosin stained photomicrographs. **a,** Histological skin sections from the pups UVB-irradiated at P1 and harvested at P7, and age-matched unirradiated control (corresponding to Figure 1d). **b,** Histological sections from subcutaneously transplanted tumors from F5061 alone and F5061 with admixed macrophages. **c,** Histological skin sections from UVB-irradiated pups (irradiated at P1, harvested at P7), administered with the indicated antibodies (corresponding to Figure 2c). Magnification 10x for all panels.

Supplementary Table 1

List of IFN-γ-specific responsive genes* among the top 20% most significantly altered genes in melanocytes at 6 days post-UVB time point

Gene Symbol	*Gene Name*	*Regulation*
Psmb8	Proteasome subunit, beta type, 8	Up
Psmb9	Proteasome subunit, beta type, 9	Up
Psmb10	Proteasome subunit, beta type, 10	Up
Ccl8	Chemokine (C-C motif) ligand 8	Up
Ciita	Class II transactivator	Up
Casp1	Caspase 1	Up
C3	Complement component 3	Up
C4a	Complement component 4a	Up
C4b	Complement component 4b	Up
Hira	Histone cell cycle regulation defective homolog A	Up
Tmod1	Tropomodulin 1	Up
Tap1	Transporter 1, ATP-binding cassette, subfamily B	Up
Tap2	Transporter 2, ATP-binding cassette, subfamily B	Up
Il7r	Interleukin 7 receptor	Up
Ctss	Cathepsin S	Up
Ccl5	Chemokine (C-C) ligand 5	Up
Aif1	Allograft inflammatory factor 1	Up
B2m	Beta-2-microglobulin	Up
Foxp3	Forkhead box P3	Up
Serpina3g	serine peptidase inhibitor, clade A, member 3G	Up
Slc6a6	solute carrier family 6, member 6	Up
Tnfrsf1b	Tumor necrosis factor receptor superfamily, member 1B	Up
Bach1	BTB and CNC homology 1, basic leucine zipper transcription factor 1	Up

* These genes are known to be responsive to IFN-γ, but not to Type-I interferons (IFN-α and IFN-β). See ref. 7 and references therein.

Supplementary Table 2

List of primers

Gene	*Forward (F) and Reverse (R) Primers*	*Source*
Real-Time RT-PCR primers		
Klra1	F 5'-AAGATTGGGCATGGATTGAC-3' R 5'-GATAACAACATACATCCCCCA-3'	qPrimerDepot[a]
Ncr1	F 5'-GGCTCACAGAGGGACATACA-3' R 5'-GGCTGCTGTTCTCAACACCT-3'	qPrimerDepot
Ccr2	F 5'-AACAGTGCCCAGTTTTCTATAGG-3' R 5'-CGAGACCTCTTGCTCCCCA-3'	qPrimerDepot
Ccr5	F 5'-CAAGACAATCCTGATCGTGCAA-3' R 5'-TCCTACTCCCAAGCTGCATAGAA-3'	qPrimerDepot
H2-K1	F 5'-GAGCAGTGGTTCCGAGTGA-3' R 5'-GGTCTTCGTTCAGGGCGATG-3'	Primer Express[b]
H2-T23	F 5'-GACTTGGAAAGCCAGGGACAT-3' R 5'-CACGTCGCAGCCGTACATC-3'	Primer Express
18S rRNA	F 5'-CTTAGAGGGACAAGTGGCG-3' R 5'-ACGCTGAGCCAGTCAGTGTA-3'	Primer Express
Primers for Ccl8, Ifna1, Ifnb1, and Ifng were obtained from RealTimePrimers.com[c]		
Genotyping primers		
TRE-H2BGFP	F 5'-GCCACAAGTTCAGCGTGTCC-3' R 5'-GATGCCCTTCAGCTCGATCC-3'	
Dct-rtTA	F 5'-ACTAAGTAAGGATCAATTCAG-3' R 5'-TGTACTAGGCAGACTGTG-3'	

[a]These primer sequences were obtained from the qPrimerDepot database (ref. 44).
[b]These primers were designed using the Primer Express software (Applied Biosystems).
[c]Real Time Primers, LLC., Elkins Park, PA, USA.

Supplementary Table 3

List of commercially available antibodies

Antibody	*Host*	*Conjugate*	*Supplier*
Flow cytometry			
CD11b	Rat	Alexa Fluor 488	BioLegend
F4/80	Rat	Alexa Fluor 647	BioLegend
IFN-γ	Rat	PE	BioLegend
NKp46	Rat	Alexa Fluor 647	eBioscience
IgG2b Isotype	Rat	Alexa Fluor 488	BioLegend
IgG1 Isotype	Rat	PE	BioLegend
IgG2a Isotype	Rat	Alexa Fluor 647	BioLegend
IgG Isotype	Hamster		Invitrogen CALTAG
IgG1 Isotype	Mouse		BD Pharmingen
Immunohistochemistry			
IFN-γ (human)	Rabbit		Lifespan Biosciences
IFN-γ (mouse)	Rabbit		Lifespan Biosciences
CD68	Mouse		Invitrogen
Ki-67	Rabbit		Epitomics
CD49b	Rat		BioLegend
CD11b	Rat		BD Pharmingen
F4/80	Rat		BioLegend
CD8a	Rat		BD Pharmingen
CD19	Rat		BD Pharmingen
CD4	Rat		BD Pharmingen
CD3e	Arm. Hamster		BD Pharmingen
CD11c	Arm. Hamster		BD Pharmingen
Gr-1	Rat		BD Pharmingen
CD16/32	Rat		BioLegend
Ctla4	Syr. Hamster		BioLegend
Others			
HRPN IgG1	Rat		BioXcell
LIVE/DEAD Fixable	Dead cell stain kit		Invitrogen